Multicriteria materials selection for extreme operating conditions based on a multiobjective analysis of irradiation embrittlement and hot cracking prediction models

Abstract

A methodology for evaluating different combinations of materials specifications for extreme environment applications is presented. This new approach addresses the materials selection problem using a multicriteria stringency level methodology that defines several thresholds obtained by analyzing different prediction models of irradiation embrittlement and hot cracking. To solve the conflicts among thresholds as provided by the different prediction models, a multiobjective approach is carried out. Materials for reactor pressure vessels have been considered as case study. It has been concluded that the best option to manufacture a pressure vessel for a pressurized water modern reactor is the selection of German manufacturing standards. Finally, a sensitivity analysis of the proposed methodology has been performed to evaluate the divergences between the single stringency level methodology and the new proposal including multicriteria decision making (MCDM) aspects.

Keywords: Prediction-model · multiobjective · MCDM · stringency level · structural materials · extreme environment

List of symbols and acronyms

A_{ij}	Requirement *i* specified by the materials specification *j*
A^+	Ideal solution
A^-	Anti-ideal solution
ASME B&PV	American Society of Mechanical Engineers Boiler & Pressure Vessels
CF	Chemical factor (R.G. 1.99 Rev.2 prediction model)
C_j^+	Relative closeness of each material requirement *Rij* to the ideal solution A^+
d_i^+	Separation between the requirement i specified by the materials specification j (*Aij*) and the ideal solution according to the constraints
d_i^-	Separation between the requirement i specified by the materials specification j (A_{ij}) and the anti-ideal solution according to the constraints
DBT	Ductile-Brittle Transition
DV	Decision variable
erf	Error function
IASCC	Irradiation-Assisted Stress Corrosion Cracking
KTA	Kern Technischer Ausschuss (German safety council)
L_i	Distance between the solution provided by the upper bounds and the medium point or requirements range as established by multiobjective approach
L_s	Standardized limit (method of Stringency Levels)
MCDM	Multicriteria Decision Making
OF	Objective function
PWR	Pressure Water Reactor
RCC – MR	French code
R.G.	Regulatory guide (United States Nuclear Regulatory Commission)
r_{ij}	Normalized stringency level
r_j	Mean value of r_{ij} for the materials specification *j*
SI_i	Sensitivity index of the output
S_j^+	The minimum Euclidean distance of any requirement of the materials specification j from the ideal solution.
S_j^-	The maximum Euclidean distance of any requirement of the materials specification j from the anti-ideal solution.
SL	Stringency Level
$SL_{(Max)}$	Maximum value of Stringency Level according to the defined scale
T_r	Threshold
Y_p	Yield Point
σ_t, σ_l	Membrane theory stresses (transversal and longitudinal components)
P	Pressure (in-service)
R, t	Radius, thickness of vessel
ϕ	Neutron flux (n/cm^2)
ΔRT_{DBT}	Shift of ductile-to-brittle transition temperature
η^*_{max}	Structural safety factor to avoid permanent local plastic deformation

1 Introduction

Broadly, materials selection is the task that comprises the translation of product requirements into material properties, followed by screening and ranking methods to find the good materials to do the job (Leite et al 2015). Material selection for any engineering component or product, in general, is subject to various constraints and fulfillment of certain goals of design (Chauhan 2015). When the choice of material is limited to a list of pre-

defined candidates, one difficulty found is that properties of different candidate materials (alternatives) may not indicate any obvious correlation in the given list (Milani and Shanian 2006). Lately, the requirement for increased efficiency and reduced costs of power plant piping systems has led to the need for advanced structural integrity assessment of new and in-service exposed welds (Hyde and Sun 2009).

The reliability of a structural system may be estimated at two levels: the component level and the system level (Jiang 2017). Thus the most important system of a nuclear power plant is the primary loop and its most relevant structural component is the reactor pressure vessel, which is manufactured primarily from ferritic steels that face specific impurity content requirements (Rodríguez-Prieto et al. 2016). The manufacturing process of a pressure vessel for a pressurized water reactor (PWR) is based on the constraints provided by manufacturing codes or standards. Modern designs of PWR pressure vessels are usually made of forged components with a cladding of austenitic stainless steels to avoid corrosion (Rodríguez et al, 2015). In order to extend the lifetime of nuclear reactors it is necessary to assess their actual technical state considering mechanical properties degradation not only for designed lifetime, but also for the period of time that is being extended (Timofeev 2003). Advanced pressure vessel materials with high strength and toughness are needed for an optimization of the design and construction, as well as the long-term operation (Kim et al. 2015).

In this work, an evaluation of requirements of chemical composition and mechanical properties has been performed. Thus, a methodology for selecting a combination of materials specifications to manufacture reactor pressure vessels is presented. This new approach considers the evaluation of materials requirements using a multicriteria stringency level methodology that uses several thresholds obtained by analyzing different prediction models of irradiation embrittlement and hot cracking on low alloy steels and austenitic stainless steels operating in the reactor environment. Finally, a sensitivity analysis is performed, assessing on the suitability of the integration of multicriteria concepts into a stringency level methodology.

2. Methodology description and theoretical approach

The selection of materials for the construction of the primary loop of a light water reactor is a complex process that involves great responsibility because small differences in chemical composition can adversely affect in-service behavior of the material (Rodríguez-Prieto et al 2017a). The vessel of a nuclear reactor is a cylindrical component (IAEA, 2011) constructed using low alloy steels with a inner cladding of austenitic stainless steels to avoid corrosion processes (Riou et al 2004; Rodríguez et al. 2015). The thickness of the reactor vessel is around 200 to 300 mm (Fig. 1), being the thickness of cladding between 2 and 10 mm (Gillemot, 2010). Mainly, the ferritic material will experience weakening due to irradiation embrittlement along with the service conditions. Whereas the inner cladding can be affected by hot cracking, fatigue and irradiation-assisted stress corrosion cracking (IASCC).

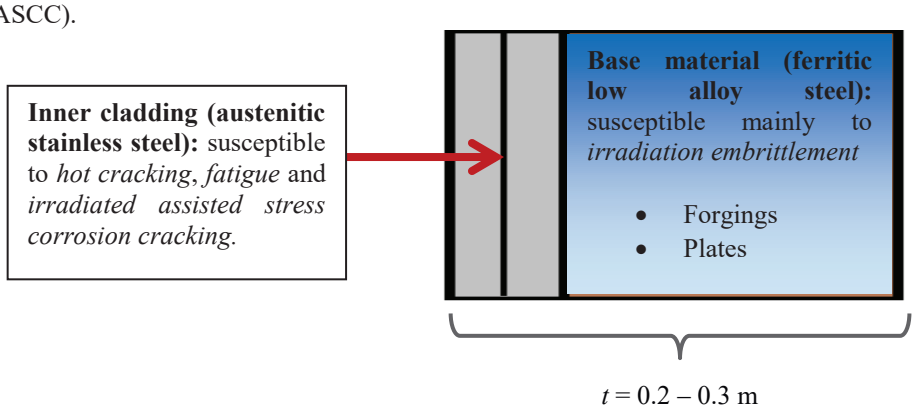

Fig. 1 Materials for reactor pressure vessel manufacturing

This research is performed (Fig. 2) by making a pre-selection of different candidate materials (Stage A) and a preliminary assessment for different irradiation embrittlement prediction models, as well as a selection of thresholds for chemical composition requirements by a multiobjective approach (Stage B). Since different embrittlement and fracture prediction models provide different constraints and upper bounds when the requirements from materials specifications are analyzed, the use of a multiobjective approach has been necessarily considered to solve the conflicts generated when all prediction models are applied jointly to get thresholds that meet the requirements of each prediction model separately and ensure that the material can be furthermore adequately evaluated versus these key thresholds.

Furthermore, different mechanical properties and materials requirements are evaluated (Stage C) by using a stringency level methodology combined with a multicriteria decision making approach (Fig. 2). Finally, a sensitivity analysis of the multicriteria assessment is performed (Stage D).

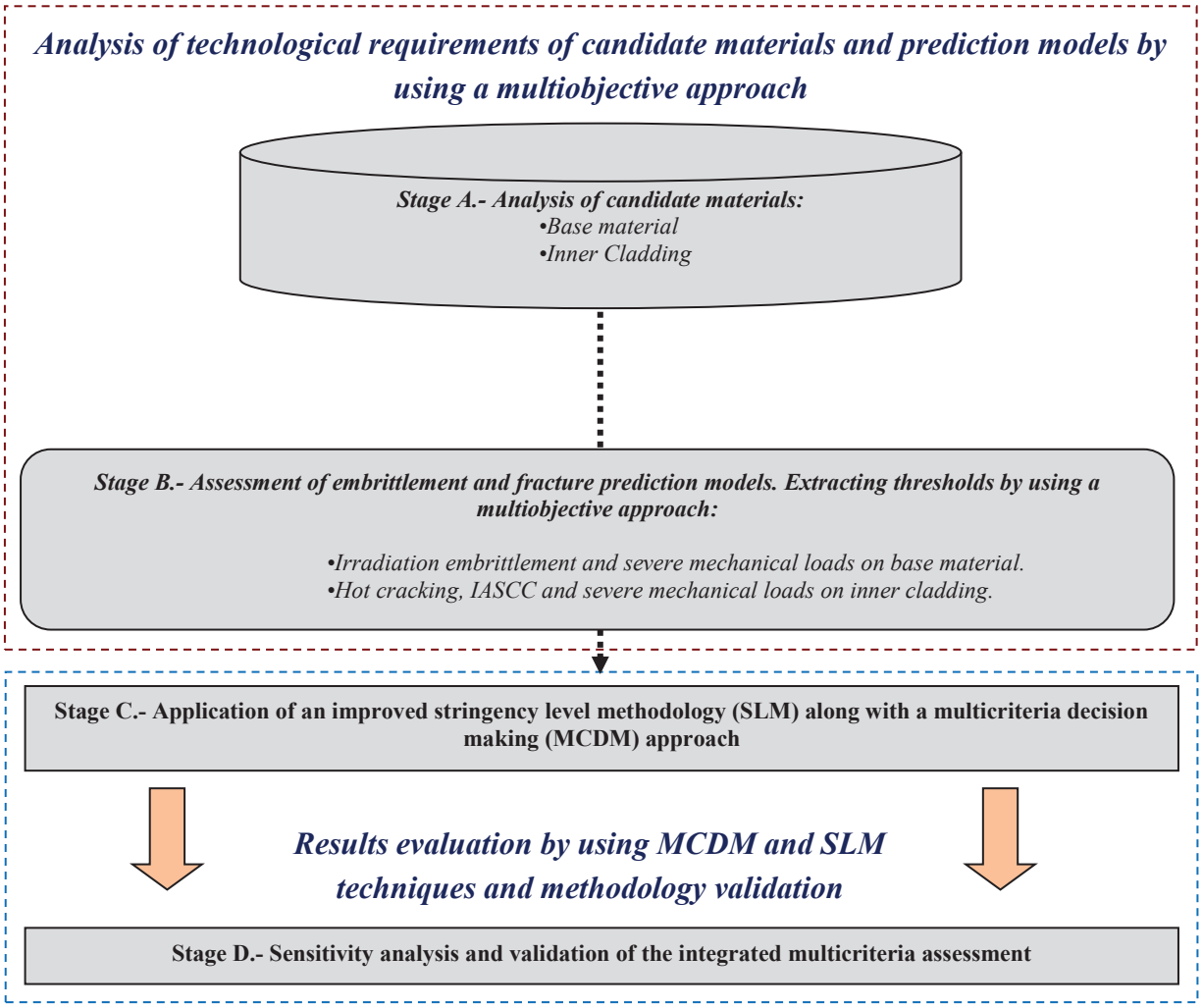

Fig. 2 Multicriteria and multiobjective approach for selecting candidate materials for RPV manufacturing

The different stages are developed as follows.

2.1 Stage A.- Analysis of candidate materials: Technological requirements for materials selection

Irradiation embrittlement is a complex phenomenon that depends on chemical composition, neutron flux, operation temperature (Soneda et al. 2011; Kirk 2013), vessel manufacturer, weld flux type, and product form (Jenkins 1993). Copper, phosphorous and nickel content are the most influential parameters (Rodríguez-Prieto et al. 2016). Steels with low carbon content and low levels of impurity are well considered to be used in the current light water reactor pressure vessels (RPV) steels and for the new generation nuclear systems (Blagoeva et al. 2014). Copper-rich precipitates have been recognized as contributing to radiation hardening in irradiated alloys, which act as barriers to the dislocation motion on the slip plane (Kwon et al. 2003).

Wu and Cao (2013) observed two mechanisms in the initial stage of the ductile-brittle transition (DBT) region: transgranular cleavage fracture and intergranular. Fujji et al. (2010) confirmed by transmission electron microscopy (TEM) imaging that dislocation loops and clusters of solute are formed in the irradiated material, whereas Kemp et al. (2006) proposed an artificial neural network to model the irradiation hardening of low-activation ferritic steels.

A model analysis for Cu-rich precipitates and an empirical logarithmic law for relaxation of residual stress demonstrated that an increment of the embrittlement due to Cu-rich precipitates increases with Cu and Ni contents and is in proportion to a yield stress change, which is related to irradiation hardening (Kobayashi et al., 2012).

While irradiation embrittlement affects the base material, other damage mechanisms affect the austenitic steels of the inner cladding. Experimental results have shown that Irradiation-Assisted Stress Corrosion Cracking

(IASCC) is dramatically increased when the sulphur content is greater than 0.03% (Chung et al., 2003). In addition, stainless steels with (P+S) < 0.03% and a δ-ferrrite wt% content greater than 4 are not susceptible to solidification cracking either (Arantes and Trevisan, 2007).

Under extreme loading conditions, the materials experience permanent deformations where they pass the elastic zone (Sharifian 2017). Thus, to evaluate the suitability of mechanical requirements described by materials specifications for the reactor pressure vessel manufacturing is essential to perform mechanical calculations according to the operating conditions to obtain the structural safety factor, to ensure that no permanent local deformations occur.

When the vessel thickness is small compared to the radius ($R_m/t > 10$), the membrane stress theory can be used (Moss and Basic, 2013). Membrane stress for cylindrical vessels can be divided into longitudinal and transversal components, obtained from Eqs. (1) and (2) (Rodríguez-Prieto et al, 2017b):

$$\sigma_l = \frac{P \cdot R}{2t} \tag{1}$$

$$\sigma_t = \frac{P \cdot R}{t} \tag{2}$$

Therefore, the structural factor can be calculated according to Eq. (3).

$$\eta = \frac{\sigma_t}{Y_P} = \frac{P \cdot R}{Y_P \cdot t} \tag{3}$$

Thus, using a design pressure (P) equal to 180 kg/cm^2, a radius of vessel (R) of 2.32m and an average thickness (t) of 0.245 m, the membrane stresses are obtained: σ_l=85.22 MPa for the longitudinal component and σ_t=170.44 MPa for the transversal component.

Table 1 provides the materials analyzed in this work along with the requirements of copper, phosphorous and nickel requirements for the base material and the chromium, nickel, phosphorous and sulphur requirements for the inner cladding. In addition, the structural factors to avoid permanent plastic deformations (calculated using Eqs. (1), (2) and (3) according to KTA 3203 (2001) and ASME II Part D App 1 (2015) are included.

Once materials and their related weakening mechanisms due to the operating conditions are presented, the Stage B is developed to analyze different damage prediction models by a multiobjective approach to obtain several thresholds to be used in the multicriteria stringency level methodology (Stage C).

Table 1 Materials analyzed and their requirements (ASME B&PV 2015; KTA 3201.1 1998; RCC-MR 2007; Bringas 2000)

Part	Material specification	Cu wt% max	P wt% max	Ni wt% max	η and Y_p in MPa
Forging	ASME SA 533 Gr. B Cl.1	0.12	0.015	0.73	0.49; Yp=345
	JIS G-3120 SQV2A	N.S.	0.035	0.70	0.49; Yp=345
	JPB (A533B cl.1)	0.01	0.017	0.83	0.49; Yp=345
	JPC (A533B cl.1)	0.01	0.007	0.81	0.49; Yp=345
Plate	ASME SA-508 Cl.3	0.20	0.025	1.00	0.38; Yp=450
	KTA-DIN 20MnMoNi55	0.12	0.012	0.85	0.44; Yp=390
	RCC 16MND5	0.20	0.020	0.80	0.43; Yp=400
	JIS G-3204 SFVQ1A	N.S.	0.025	1.00	0.29; Yp=585
	Material specification	**Cr wt% max**	**Ni wt% max**	**P+S wt% max**	**η and Y_p in MPa**
Inner cladding	AISI 304L	20.00	10.50	0.095 (S=0.03)	0.83; Yp=515MPa
	DIN X5 Cr Ni 18-10	19.50	10.50	0.060 (S=0.015)	0.81; Yp=520MPa
	AISI 347	19.00	13.00	0.075(S=0.03)	0.83; Yp=515MPa
	DIN X6 Cr Ni Nb 18-10	19.00	12.00	0.050 (S=0.015)	0.83; Yp=510MPa

2.2. Stage B.- Assessment of material embrittlement and fracture prediction models using a multiobjective approach

In the Stage B, embrittlement and fracture prediction models for the base material and the inner cladding used in the manufacture of reactor pressure vessels are analyzed using a multiobjective approach to obtain thresholds to be used as upper bounds in the multicriteria assessment of a requirement stringency methodology. The Stage B is developed according to the diagram shown in Fig. 3.

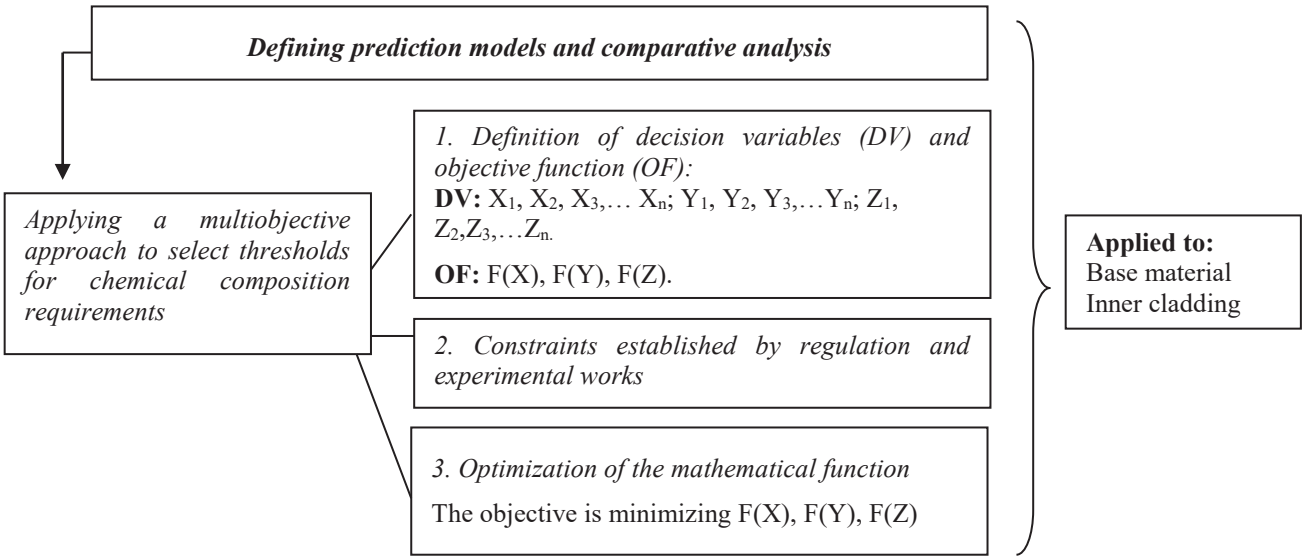

Fig. 3 Multiobjective approach to select thresholds for chemical composition requirements for the base material and the inner cladding

Fig. 3 exhibits schematically the procedure to get thresholds from the different analyzed models for predicting irradiation embrittlement (R.G. 1.99 Rev.2, NUREG CR 6551 and ASTM E900-02 models for base materials) and hot cracking (WRC-92 and De Long model for inner cladding materials) avoiding other damage mechanisms like the irradiation-assisted stress corrosion cracking (IASCC). The procedure uses several important concepts, these are as follows: decision variables (ΔRT_{DBT} and Cu wt% and Ni wt% for the base materials and the δ-Ferrite and Cr_{eq}/ Ni_{eq} wt% P+S wt% for the inner cladding materials), several constraints issued by different regulations to avoid other degradation mechanisms and the calculation of an ideal solution (to ensure the considered degradation mechanisms are avoid) and an anti-ideal solution, which selection would generate damage in the material. Finally, using a representation based on matrixes (Fig. 6 and Fig.8), thresholds to avoid every degradation mechanism are proposed.

We define a multiobjective approach to solve the conflicts among thresholds as provided by different embrittlement and fracture prediction models and certain constraints as described by different regulations for base material and inner cladding. The model consists of the three following components:

- **Decision variables:** The decisions of the problem are represented using symbols such as X_1, X_2, X_3,… X_n; Y_1, Y_2, Y_3,…Y_n; Z_1, Z_2, Z_3,…Z_n. Each decision variable indicates for the base material whether or not the ΔRT_{DBT} and Cu wt% and Ni wt% are less than the upper bounds established by KTA 3203 (they are known as binary variables). Analogously, each decision variable indicates for the inner cladding whether or not the δ-Ferrite and Cr_{eq}/ Ni_{eq} wt% P+S wt% are less than the upper bounds establish by key research works and the industrial practice. The assignment function is represented in Fig. 4.

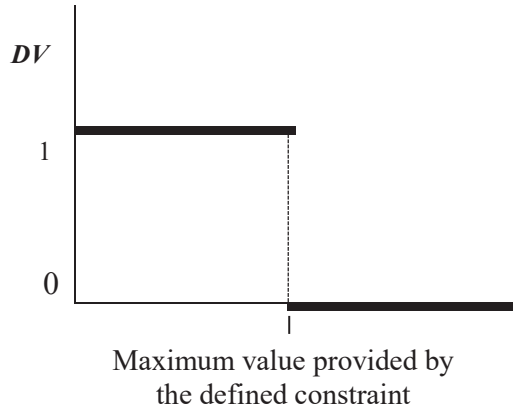

Fig. 4 Decision variables as a function of a constraint or goal in the multiobjective approach

- **Constraints:** The limitations or requirements of the problem are expressed as upper bounds as described by regulations, industrial standards or industrial experience.

- **Optimization:** The separation between the requirement i specified by the materials specification j (A_{ij}) and the ideal solution according to the constraints defined is called d_i^+. Similarly, the separation between the requirement i specified by the materials specification j (A_{ij}) and the anti-ideal solution according to the constraints defined is called d_i^-. The Eq. (4) provides the interval calculation.

$$d_i^+ + d_i^- = \left|A^+ - A_{ij}\right|, i = 1, \ldots, n;\ d_i^+, d_i^- \geq 0, \tag{4}$$

The problem therefore can be written according to Eq. (5):

$$min\ \sum_{i=1}^{n} d_i^+ + d_i^- \tag{5}$$

Thus, the approach allows to optimize the beneficial impact of applying an adequate threshold to evaluate the further in-service behavior of material.

Once defined the mathematical approach, prediction models are firstly introduced and analyzed and the multiobjective evaluation is applied. The analysis is divided into two subsections A) base material and B) inner cladding.

A) Base material

The formulas for predicting the shift of ductile to brittle transition temperature have the general expression, according to Eq. (6):

$$\Delta RT_{DBT} = A\ (Chemistry,\ Temperature,\ Flux).\ \phi^n \tag{6}$$

Table 2 shows different equations proposed by several authors from 1977 to present (Eqs. 7-15).

Table 2 Irradiation embrittlement prediction models (Ballesteros and Acosta 1997; R.G. 1.99 Rev.1 1977; R.G. 1.99 Rev.2 1988, Eason et al 1998; ASTM E900-02 2002)

Prediction model	Equation	
R.G. 1.99 Rev.1 (1977)	ΔRT_{DBT} (ºF) =[40 + 1000(Cu - 0.08) + 5000 (P -0.008)] · [$\phi/10^{19}$]$^{1/2}$ *Limitation:* Do not consider Ni wt%	(7)
Odette et al. (1984)	ΔRT_{DBT} (°C) = 200·Cu·(1+1.38(erf (0.3·Ni-Cu)/Cu)+1) · (1-e$^{(-\phi/0.11))^{1.36}}$ ϕ^{18}	(8)
R.G. 1.99 Rev.2 (1988)	ΔRT_{DBT} (°F) = (CF) · f (0.28 – 0.10 log f) *Parameters for calculation:* CF provided in a table (RG 1.99 Rev.2) up to Cu≤0.4 and Ni≤1.2.	(9)
Miannay et al. (1993)	ΔRT_{DBT} (°C) = 10.98 + 316.4·(P- 0.008) + 225.29·(Cu – 0.08) + 12.10·(Ni – 0.7) + 248.31 · (Cu – 0.08) ·(Ni – 0.7)) · $\phi^{0.70}$	(10)
RCC-M Code	ΔRT_{DBT} (°C) = 22+556 (%Cu-0,08)+2778 (%P-0,008)] · [$\phi/10^{19}$]$^{1/2}$ Limitation: neutron fluences between 1.10^{18} and 6 10^{19} n/cm^2;	(11)
JEPE (Japan)	ΔRT_{DBT} (°C) = (-16 + 1210·P + 215·Cu+ 77·(Ni ·Cu)$^{1/2}$) · $\phi^{0.29 - 0.04}$ logϕ	(12)
PNAE (Russia)	ΔRT_{DBT} (°C) = (575· (P + 0.1 Cu)+20) · (18 . ϕ)$^{1/3}$ Limited to: WWER-1000 (T= 290 °C), High Ni	(13)
NUREG CR-6551 (1998)	ΔRT_{DBT} (°F) = A·exp [$C_{Tc}/(T_c + 460)$] · [1 + $C_P P$] (φt)$^{\alpha}$ + B · [1 + $C_{Ni} Ni^{\eta}$] F(Cu) · G(φt)+ Bias *Recommended parameters for calculation:* $A_{forging}$= 9.3 x 10^{17}; A_{plates}= 12.7 x 10^{17}; $C_{Tc=}$ 1.93 x 10^4; T_c (ºF)= 572 ºF (300ºC); C_P=110; P(wt%)=0.02; Φt=1-5 x 10^{19}; α=0.4601; $B_{forging}$=132; B_{plates}=156; C_{Ni}=2.4; Ni (wt%)=0-1.2; η=1.250; κ=0.659; Cu_{th}=0.072; Cu (wt%)=0-0.4; $C_{t=}$4.58 x 10^{12}; μ=18.265; σ=0.713; t_f (h)= 360000.	(14)
ASTM E900-02	ΔRT_{DBT} (°F)= A·exp [$C_{Tc}/(T_c + 460)$] [1 + $C_P P$] (φt)$^{\alpha}$ + B [1 + $C_{Ni} Ni^{\eta}$] F(Cu) G(φt) *Recommended parameters for calculation:* $A_{forging}$= 6.7 x 10^{18}; A_{plates}= 6.7 x 10^{18}; $C_{Tc=}$ 2.07 x 10^4; T_c (ºF)= 572 ºF (300ºC); C_P=0; P(wt%)=0.02; Φt=1-5 x 10^{19}; α=0.5076; $B_{forging}$=128; B_{plates}=156; C_{Ni}=2.106; Ni (wt%)=0-1.2; η=1.173; κ=0.577; Cu_{th}=0.072; Cu (wt%)=0-0.4; $C_{t=}$0; μ=18.24; σ=1.052; t_f (h)= 360000.	(15)

Notes: ϕ=neutron flux (n/cm^2). f=neutron flux/10^{19} (n/cm^2). erf=error function. erf(x) = $\frac{2}{\sqrt{\pi}} \int_0^x e^{-t^2}\, dt$;

Nowadays, the most consolidated and used models are R.G. 1.99 Rev.2, NUREG CR 6551 and ASTM E 900-02, along with the KTA 3203 (2001) that provides the ductile-to-brittle transition temperature (ΔRT_{DBT}) in graphic form. Thus, Fig. 3 shows how the three models provide different Cu-Ni relationship to avoid maximum value for (ΔRT_{DBT}) equal to 40ºC as provided by KTA 3203. Fig. 5 exhibits the upper bounds map for irradiation embrittlement immunity as a function of Cu and Ni wt% according to the R.G. 1.99 Rev.2 (1988), NUREG CR 6551 (Eason et al. 1998) and the ASTM E900-02 (2002) prediction models.

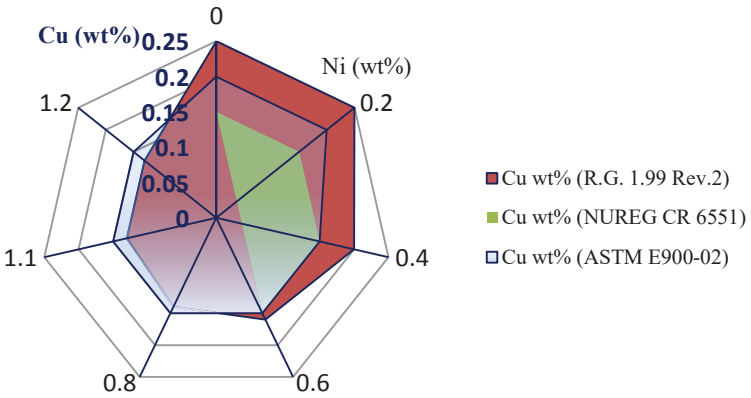

Fig. 5 Upper bounds map for irradiation embrittlement immunity as a function of Cu and Ni wt% according to the R.G. 1.99 Rev.2, NUREG CR 6551 and the ASTM E900-02 prediction models

Then, the multiobjective approach is applied for the analysis of requirements to avoid irradiation embrittlement:

Decision variables and constraints:

X_{ij}= 1, if the ΔRT_{DBT} of the material *i* according to the prediction model *j* is less than 40ºC as established by KTA 3203, and X_{ij} = 0 otherwise.
Using Eqs. (9), (14) and (15) as provided in Table 2, Table 3 shows the ΔRT_{DBT} for a composition variable between 0.10 and 0.25 wt% for copper and 0 and 1.2 wt% for nickel.

Table 3 Ductile-to-brittle transition temperature shift (ΔRT_{DBT}) according to R.G. 1.99 Rev.2, NUREG CR 6551 and ASTM E900-02.

Cu wt % content	ΔRT_{DBT}	Ni wt% content						
		0	**0.2**	**0.4**	**0.6**	**0.8**	**1**	**1.2**
0.10	R.G. 1.99	5.00	14.44	18.33	18.33	19.44	19.44	19.44
	NUREG	10.27	11.17	12.41	13.82	15.35	16.99	18.71
	ASTM	4.8	5.9	7.28	8.8	10.4	12.08	13.81
0.12	R.G. 1.99	9.44	19.44	26.11	28.33	30.00	30.00	30.00
	NUREG	20.01	21.3	23.06	25.07	27.26	29.59	32.04
	ASTM	17.71	19.44	21.61	23.98	26.5	29.14	31.86
0.15	R.G. 1.99	16.11	26.67	37.22	43.33	46.11	47.22	47.22
	NUREG	32.29	34.05	36.48	39.26	42.27	45.48	48.86
	ASTM	23.01	24.99	27.49	30.23	33.12	36.14	39.27
0.17	R.G. 1.99	20.56	31.11	43.33	52.78	55.56	57.22	57.22
	NUREG	39.57	41.62	44.45	47.67	51.17	54.90	58.82
	ASTM	35.8	38.41	41.68	45.27	49.07	53.04	57.16
0.20	R.G. 1.99	27.78	38.89	51.67	65.00	70.56	73.33	73.89
	NUREG	49.6	52.04	55.42	59.25	63.43	67.88	72.56
	ASTM	36.5	39.15	42.46	46.1	49.95	53.98	58.14
0.22	R.G. 1.99	32.78	44.44	56.67	71.67	80.00	82.78	84.44
	NUREG	55.84	58.53	62.24	66.46	71.06	75.96	81.11
	ASTM	50.18	53.49	57.65	62.2	67.02	72.06	77.28
0.25	R.G. 1.99	40.00	52.22	64.44	80.00	92.78	97.78	101.11
	NUREG	64.69	67.73	71.91	76.68	81.87	87.41	93.22
	ASTM	47.88	51.08	55.09	59.49	64.15	69.01	74.05

If the RPV is not designed and manufactured according to KTA 3201.1 (1998) and KTA 3201.3 (2007), the standard KTA 3203 (2001) establishes overall the following restrictions, in Eq. (16), for copper and nickel contents (wt %).

$$KTA\ 3203 = \begin{cases} Cu \leq 0.15\%, & \forall\ 0 < Ni \leq 1.1 \\ Ni \leq 1.1\%, & \forall\ 0 < Cu \leq 0.15 \end{cases} \quad (16)$$

For a neutron fluence equal to 1 10^{19}n/cm^2, using a maximum value of Phosphorous equal to 0.02 wt% (Amayev 1993) the maximum ΔRT_{DBT} specified by KTA 3203, i.e. 40 ºC, the upper bounds for copper and nickel are shown in Eqs. (17), (18) and (19).

$$R.G.\ 1.99\ Rev.2 = \begin{cases} Cu \leq 0.25,\ \forall\ 0 < Ni \leq 0.2 \text{ and } \forall P\ (wt\%) \\ Cu \leq 0.20,\ \forall\ 0.2 < Ni \leq 0.4\ \forall P\ (wt\%) \\ Cu \leq 0.16,\ \forall\ 0.4 < Ni \leq 0.6\ \forall P\ (wt\%) \\ Cu \leq 0.14,\ \forall\ 0.6 < Ni \leq 0.8\ \forall P\ (wt\%) \\ Cu \leq 0.13,\ \forall\ 0.8 < Ni \leq 1.2\ \forall P\ (wt\%) \end{cases} \quad (17)$$

$$NUREG\ CR\ 6551 = \begin{cases} Cu \leq 0.15,\ \forall\ Ni < 0.6 \text{ and } P < 0.02\ (wt\%) \\ Ni\ wt\%\ max = 0.6. \end{cases} \quad (18)$$

$$ASTM\ E900\text{-}02 = \begin{cases} Cu \leq 0.2,\ \forall\ Ni < 0.2 \quad \text{and } P < 0.02\ (wt\%) \\ Cu \leq 0.15,\ \forall\ 0.2 \leq Ni < 1.2 \text{ and } P < 0.02\ (wt\%) \end{cases} \quad (19)$$

Analyzing the upper bounds provided by R.G. 1.99 Rev.2, NUREG CR 6551 and ASTM E900-02 prediction models, the thresholds are calculated using the multiobjective approach.

Thresholds calculation:

Using the criterion of X_{ij}= 1 if the $\Delta RT_{DBT} \leq$ 40ºC as established by KTA 3203, and X_{ij} = 0 otherwise, the following matrixes of results (Fig. 6) are obtained meeting the requirements from R.G. 1.99 Rev.2, NUREG CR 6551 and ASTM E900-02 prediction models.

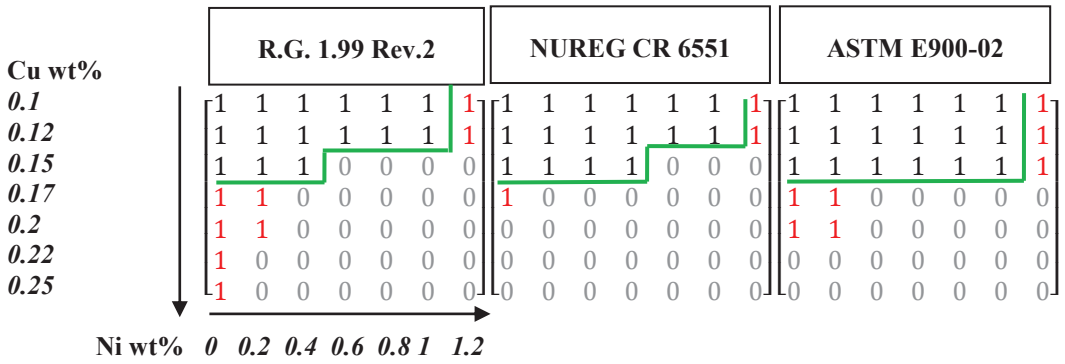

Note: green line limits the copper and nickel wt% content that according to R.G. 1.99 Rev.2, NUREG CR 6551 and ASTM E900-02, meets the constraints provided by KTA 3203.

Fig. 6 Matrixes for threshold calculation (base material)

The values marked in red color do not meet the constraints provided by KTA 3203.

B) Inner cladding

Small amount of δ-ferrite in the austenite reduce hot cracking (Moorhead *et al* 1979). Additionally, a small amount of δ-ferrite mitigates the harmful effect of sulphur atoms trapped in the ferrite (Chung *et al* 2003). Several studies have focused on solidification mode prediction and estimation of the amount of δ-ferrite in stainless steels. In fact, the δ-ferrite content (%wt) can be estimated using well-recognized predictive methods

(Valiente 2012). These prediction models are based on the concepts of chromium and nickel equivalents calculated from the %wt of the most influential elements (Rodríguez Prieto et al., 2017c).

The Eqs. (20) and (21) for the calculation according to the De Long diagram according to KTA 3201.1 (1998).

$$Cr_{eq} = Cr + Mo + 1.5Si + 0.5Nb \quad (20)$$

$$Ni_{eq} = Ni + 0.5Mn + 30C + 30N \quad (21)$$

The Eqs. (22) and (23) used by the WRC prediction (Kotecki and Siewert, 1992) model are shown below:

$$Ni_{eq} = Ni + 35C + 0.25Cu \quad (22)$$

$$Cr_{eq} = Cr + Mo + 0.7\,Nb. \quad (23)$$

The WRC-92 and the DeLong diagrams provide the ferrite number (FN), coincides with the %wt content of δ-ferrite up to a FN equal to 6 (ASM, 2012). Thus, using the diagrams of WRC (Kotecki and Siewert, 1992) and the DeLong (KTA 3201.1, 1998) prediction models, Fig. 7 provides the map for hot cracking immunity as a function of Ni_{eq} and Cr_{eq}. The immunity zone has been selected for a δ-Ferrite wt% between 5 and 15.

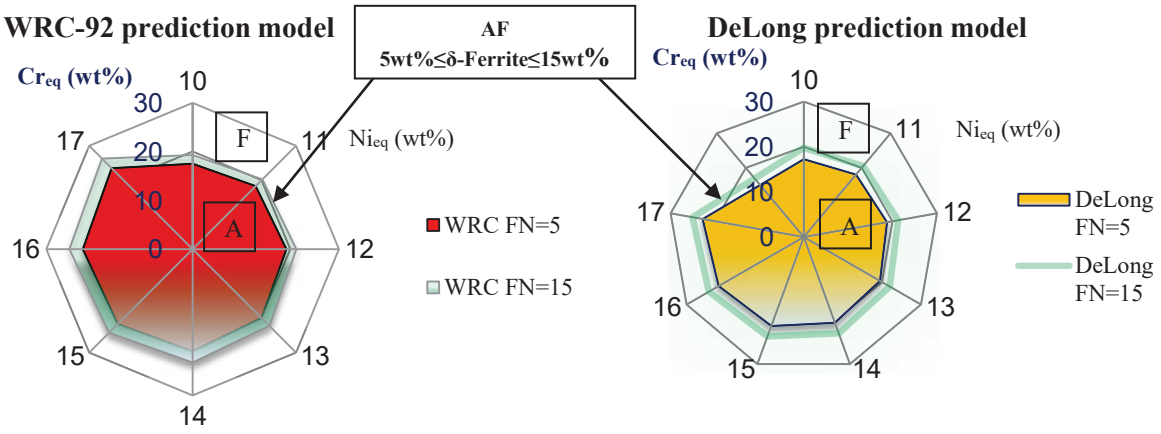

Notes: A- Austenitic structure; F-Ferritic structure; AF-Austenitic structure with a δ-Ferrite wt% between 5 and 15.

Fig. 7 Comparative map for hot cracking immunity as a function of Ni_{eq} and Cr_{eq} according to WRC-92 (a) and DeLong (b) prediction models

The change in the solidification mode from primary austenite (AF) to primary ferrite (FA) occurs at a Cr_{eq}/Ni_{eq} ratio between 1.4 and 1.5. Values $1.5<Cr_{eq}/Ni_{eq}<1.9$ correspond to the FA mode. A Cr_{eq}/Ni_{eq} ratio greater than 2 also corresponds with a ferritic solidification mode (Welding Handbook 2014).

Then applying the multiobjective approach, the following components are obtained:

Decision variables and constraints: X_{ij} = 1, if the *FN* of the *material i* according to the *prediction model j* is between 5-15, and X_{ij} = 0 otherwise. Table 4 exhibits the Ferrite Number provided by the WRC-92 and the DeLong hot cracking prediction models.

Table 4 Ferrite Number (δ-Ferrite) according to the WRC-92 and the DeLong prediction models.

Ni_{eq} wt % content	Cr_{eq} wt% content			
	WRC-92 FN=5	WRC-92 FN=15	DeLong FN=5	DeLong FN=15
10	17.5	19.25	17.25	19.75
11	18.25	20.25	18.00	20.50
12	19.25	21.25	18.75	21.25
13	20.00	22.25	19.5.0	22.00
14	21.00	23.25	20.25	22.75
15	21.75	24.25	21.00	23.50
16	22.50	25.25	21.75	24.25
17	23.50	26.25	22.75	25.00

The constraints applied at the threshold problem selection are according to Eqs. (24), (25) and (26).

$$Corrosion\ Tolerance = \begin{cases} Cr \geq 12wt\% \\ Ni \geq 8wt\% \end{cases} \tag{24}$$

Experimental results have shown that Irradiation-Assisted Stress Corrosion Cracking (IASCC) is dramatically increased when the Sulphur content is greater than 0.03% (Chung et al. 2003).

$$Irradiated\ Stress\ Corrosion\ Cracking = \begin{cases} S \leq 0.03wt\% \end{cases} \tag{25}$$

A δ-Ferrite content provided by a FN between 5 and 15 is suitable to avoid hot cracking in the stainless steels used in the inner cladding of a reactor pressure vessel. Phosphorus and sulphur decrease resistance to hot cracking (Rodríguez et al. 2015). In addition, Brooks and Thompson (1991) proposed that Cr_{eq}/Ni_{eq} ratios greater than 1.5 render the metal immune to hot cracking.

$$Hot\ cracking\ protection = \begin{cases} 5 \leq FN \leq 15 \\ (P+S)\ wt\% \leq 0.03 \\ Cr_{eq}/Ni_{eq} \geq 1.5 \end{cases} \tag{26}$$

According to these constraints, Eqs. (27) and (28) show the recommendable chromium and nickel equivalent to enhance δ-Ferrite content (FN) between 5 and 15wt%.

$$De\ Long = \begin{cases} 17 < Creq \leq 18.5,\ \forall\ 12 \leq Nieq < 14\ (wt\%) \\ 18.5 < Creq \leq 20.5,\ \forall\ 14 \leq Nieq < 16\ (wt\%) \\ 20.5 < Creq \leq 22.5,\ \forall\ 16 < Nieq < 18\ (wt\%) \end{cases} \tag{27}$$

$$WRC\text{-}92 = \begin{cases} 17 < Creq \leq 18.5,\ \forall\ 12 \leq Nieq < 14\ (wt\%) \\ 18.5 < Creq \leq 20.5,\ \forall\ 14 \leq Nieq < 16\ (wt\%) \\ 20.5 < Creq \leq 22.5,\ \forall\ 16 < Nieq < 18\ (wt\%) \end{cases} \tag{28}$$

Analyzing the upper bounds provided by the WRC-92 and the De Long prediction models, the thresholds are calculated using the multiobjective approach.

Thresholds calculations:

Using the criterion of $X_{ij} = 1$, if the FN of the *material i* according to the *prediction model j* is between 5-15, and $X_{ij} = 0$ otherwise, the following matrix of results (Fig. 8) are obtained for the WRC-92 and the De Long prediction models

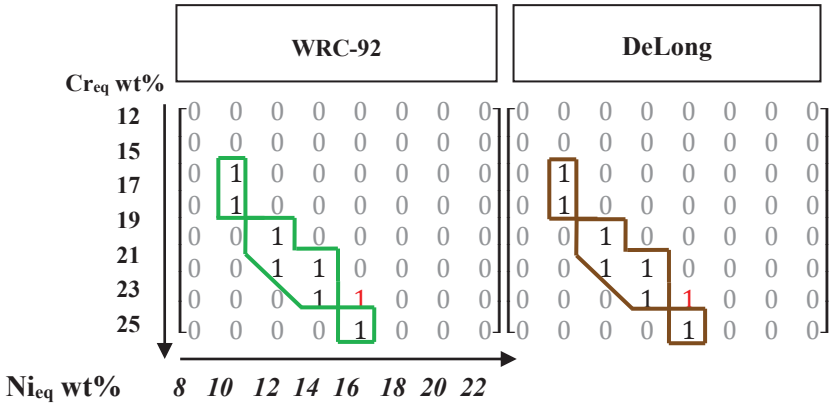

Note: green and brown lines limit the Chromium equivalent and Nickel equivalent (wt%) content that according to the WRC-92 and the DeLong prediction models, meets the constraints: $Cr_{eq}/Ni_{eq} \geq 1.5$ and $5 \leq FN \leq 15$.

Fig. 8 Matrixes for threshold calculation (inner cladding)

The values marked in red color do not meet the constraints provided by Eqs. (24), (25) and (26).

In summary, Table 5 provides the thresholds proposed, analyzing the different prediction models for the base material and the inner cladding by the proposed multiobjective approach.

Table 5 Thresholds obtained and their constraints

Base material (Forging and plates)				Inner Cladding			
Cu max wt%	**Ni wt%**	**P wt%**	**η max***	**Cr_{eq}/Ni_{eq}**	**FN**	**(P+S) wt%**	**η max***
0.15 ∀ Ni wt%<0.6 0.12 ∀ 0.6≤Ni wt%<1	1 ∀ Cu wt%<0.12	0.02	0.67	1.5-1.9	5-15	0.03	0.90

Notes: η-structural safety factor
* According to KTA 3201.2 (2011) and ASME B&PV II D App. 1 mandatory (2015).

Once, the prediction models for the base materials and the inner cladding are analyzed and the thresholds are calculated, the multicriteria stringency level methodology is applied (Stage C as follows).

Stage C.- Application of an improved stringency level methodology (SLM) along with a multicriteria decision making (MCDM) approach

Stringency level methodology (SLM) is a suitable tool for selecting materials for high demanding applications. This methodology assigns several stringency levels for each chemical requirement of materials (Rodríguez et al. 2016, 2017a). Fig. 9 establishes the stringency level assignation for each requirement of the base material as a function of the distance between the requirement and the thresholds calculated in the Stage B.

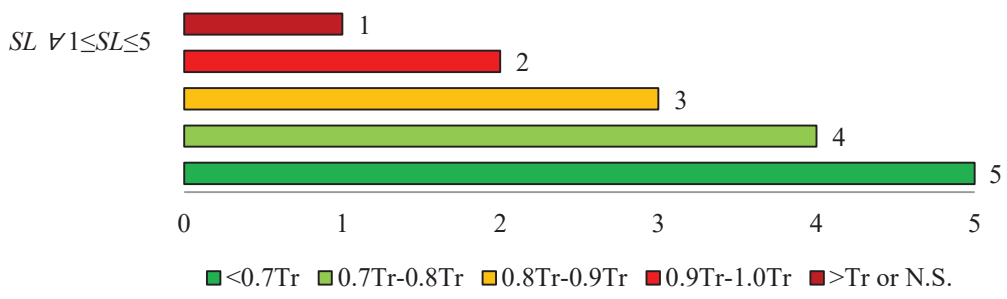

Notes: T_r-Threshold obtained by multiobjective approach evaluating embrittlement and fracture prediction models (indicated in Table 5)

Fig. 9 Stringency level assignation for the requirements of the base material

On the other hand, Fig. 10 provides the stringency level assignation as a function of the values of Cr_{eq}-Ni_{eq} ratio and δ-Ferrite (FN).

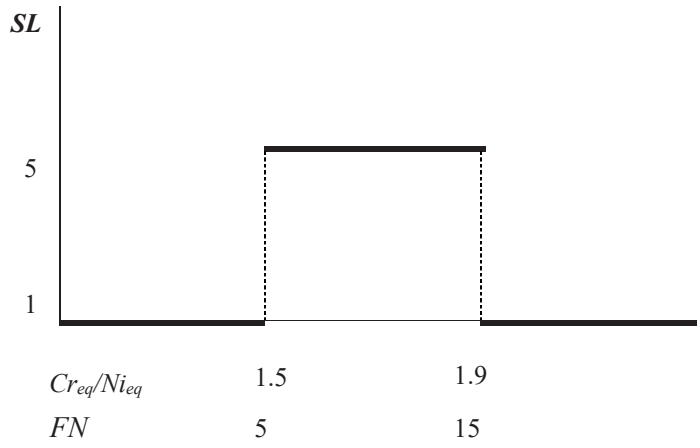

Fig. 10 Stringency level assignation for the inner cladding requirements

Using the assignations provided the stringency level methodology (Fig. 9 and 10), Table 6 shows the stringency levels for the requirements analyzed for the case study materials.

Table 6 Stringency level evaluation

Material	SL (Cu wt%)	SL (Ni wt%)	SL (P wt%)	SL (η)	Total
Forgings					
ASME SA 533 Gr. B Cl.1	2	4	4	4	14
JIS G-3120 SQV2A	1	5	1	4	11
JPB (A533B cl.1)	5	3	3	4	15
JPC (A533B cl.1)	5	3	5	4	17
Plates					
ASME SA-508 Cl.3	1	2	1	5	9
KTA-DIN 20MnMoNi55	2	3	5	5	15
RCC 16MND5	1	3	2	5	11
JIS G-3204 SFVQ1A	1	2	1	5	9
Inner cladding					
	SL (Cr_{eq}/Ni_{eq} wt%)	SL (FN)	SL (P+S wt%)	SL (η)	
AISI 304L	1	1	1	2	5
X5 Cr Ni 18-10	1	1	1	2	5
AISI 347	1	1	1	2	5
DIN X6 Cr Ni Nb 18-10	5	5	1	2	13

Since stringency level methodology only considers the location of values and not the dispersion in the calculation of the relative closeness to an ideal solution, dispersion is included developing a multicriteria approach. Thus, once obtained the stringency levels (Table 6), the normalization of criteria values are carried out using a normalization vector. The normalized value r_{ij} is calculated by Eq. (29):

$$r_{ij} = \frac{SL_{ij}}{\sqrt{\sum_{i=1}^{M} SL_{ij}^2}} \tag{29}$$

Where SL_{ij} represents the stringency level of i-requirement for j-material, r_{ij} represents the value of the new normalized decision-making matrixes.

The multicriteria evaluation of alternatives problem is usually defined by criterion matrix as follows:

$$\begin{bmatrix} y_{11} & y_{12} & \cdots & y_{1k} \\ y_{21} & y_{22} & \cdots & y_{2k} \\ \vdots & & \ddots & \\ y_{n1} & y_{n2} & \cdots & y_{nk} \end{bmatrix}$$

Focusing on the case study, the following multicriteria matrix considers not only the calculated values but also the dispersion among values (Fig. 11)

	Matrix A-Forgings				Matrix B-Plates				Matrix C-Inner cladding			
1	0.27	0.52	0.57	0.50	0.38	0.39	0.18	0.50	0.19	0.19	0.50	0.50
2	0.13	0.66	0.14	0.50	0.76	0.59	0.90	0.50	0.19	0.19	0.50	0.50
3	0.67	0.39	0.42	0.50	0.38	0.59	0.36	0.50	0.19	0.19	0.50	0.50
4	0.67	0.39	0.71	0.50	0.38	0.39	0.18	0.50	0.94	0.94	0.50	0.50
	r_j(Cu)	r_j(Ni)	r_j(P)	r_j(η)	r_j(Cu)	r_j(Ni)	r_j(P)	r_j (η)	r_j (Cr_{eq}/Ni_{eq})	r_j(FN)	r_j(P+S)	r_j(η)

Notes: A1-ASME SA 533 Gr. B Cl.1; A2-JIS G-3120 SQV2A; A3-JPB; A4-JPC; B1- ASME SA-508 Cl.3; B2-KTA-DIN 20MnMoNi55; B3-RCC 16MND5; B4-JIS G-3204 SFVQ1A; C1-AISI 304L; C2-X5 Cr Ni 18-10; C3-AISI 347; C4-DIN X6 Cr Ni Nb 18-10.

Fig. 11 Multicriteria matrixes showing normalized values for the materials requirements

The mean value of r_j for the specification *j* could be calculated according to Eq. (30):

$$r_j = \frac{1}{n} \sum_{i=1}^{n} r_{ij} \tag{30}$$

The multicriteria analysis requires the definition of an ideal solution (A^+), Eq. (31), and an anti-ideal solution (A^-), Eq. (32).

$$A^+ = \{(\text{Threshold } \forall \ \max r_{ij} \ | j \in J) | i = 1,2,3,\ldots,M\} = = \{r_1^+, r_2^+, \ldots, r_N^+\} \tag{31}$$

$$A^- = \{(\ \text{Threshold } \forall \ \min r_{ij} \ | j \in J) | i = 1,2,3,\ldots,M\} = = \{r_1^-, r_2^-, \ldots, r_N^-\} \tag{32}$$

Where *J* is the subset of materials contained in each classification of materials (forgings, plates and inner cladding).

Table 7 provides the ideal solution (A^+) and the anti-ideal solution (A^-) for each requirement evaluated.

Table 7 Ideal solution and anti-ideal solution

Base material (Forging and plates)				Inner Cladding			
A^+(Cu wt%)	A^+(Ni wt%)	A^+(P wt %)	A^+(η max*)	A^+(Cr_{eq}/Ni_{eq})	A^+(FN)	A^+(P+S wt%)	A^+(η max*)
Max 0.11 ∀ Ni wt%<0.6 Max 0.08 ∀0.6≤Ni wt%<1	0.7 ∀ Cu wt%<0.12	0.014	0.47	1.5-1.9	5-15	0.011	0.63
A^-(Cu wt%)	A^-(Ni wt%)	A^-(P wt%)	A^-(η max*)	A^- (Cr_{eq}/Ni_{eq})	A^-(FN)	A^-(P+S wt%)	A^-(η max*)
>0.15 ∀ Ni wt%<0.6 >0.12 ∀0.6≤Ni wt%<1 or N.S.	>1 ∀ Cu wt%<0.12 or N.S.	>0.02 or N.S.	≥0.67	<1.5 >1.9	<5	0.011	≥0.90

Note: NS- Not specified.

Eqs. (33) and (34) normalize to obtain r_i^- and r_i^+ using the stringency scale (according to Fig. 9 and 10).

$$r_i^+ = \frac{SL(A_{ij}^+)}{\sqrt{\sum_{i=1}^{M} SL(A_{ij}^+)^2}} \tag{33}$$

$$r_i^- = \frac{SL(A_{ij}^-)}{\sqrt{\sum_{i=1}^{M} SL(A_{ij}^-)^2}} \quad (34)$$

Therefore a mean value equal to 0.94 is obtained for r_i^+ and equal to 0.11 for r_i^-.

The separation measure of each requirement stringency level from the ideal-solution and negative-ideal solution using the n-dimensional Euclidean distance method is then calculated where Si^+ is the minimum Euclidean distance of the requirement of the materials specification j from the ideal solution, calculated by Eq. (35):

$$S_j^+ = min\sqrt{\sum_{j=1}^{n}(r_{ij} - r_i^+)^2} \quad i = 1, \dots, M \; \forall \; r_{ij} \leq r_i^+ \quad (35)$$

Whereas S_j^- is the Euclidean distance of each requirement stringency level from the anti-ideal solution, calculated by Eq. (36):

$$S_j^- = max\sqrt{\sum_{j=1}^{n}(r_{ij} - r_i^-)^2} \quad i = 1, \dots, M \; \forall \; \forall r_{ij} \geq r_j^- \quad (36)$$

Fig. 12 shows representatively the calculation of S_j^+ (a) and S_j^- (b), considering that this case study can be represented in a bidimensional space (i,j).

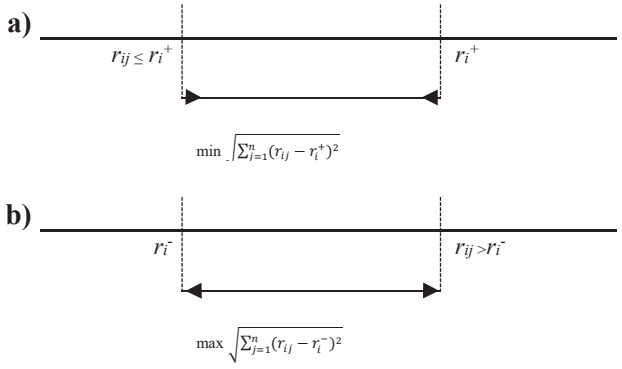

Fig. 12 Calculation of S_j^+ (a) and S_j^- (b): criteria for requirements with upper bound (base material: copper, nickel, phosphorous and structural safety factor; inner cladding: phosphorous, sulphur and structural safety factor)

The relative closeness of each material requirement r_{ij} to the ideal solution A^+ can be calculated according to Eq. (37):

$$C_j^+ = \frac{S_j^-}{|S_j^+ + S_j^-|}, 0 \leq C_j^+ \leq 1, j = 1, \dots, M. \quad (37)$$

If Cj=1 then $r_{ij} = A^+$ (ideal solution) and if Cj=0, then $r_{ij} = A^-$ (anti-ideal solution). Therefore, the conclusion is that the alternative ai is closer to A^+ if Cj is closer to the value of 1.

3 Results

The ideal solution is calculated according to the stringency level methodology functions (Fig.s 8 for the base material and Fig. 9 for the inner cladding) to obtain the maximum stringency level (SL_{max}=5), whereas the anti-ideal solution is the value of threshold to obtain the minimum assignation of SL (SL_{min}=1) as Table 7 indicates.

Table 8 provides the calculation of the relative closeness (C_j^+) to the ideal solution.

Table 8 Calculation of the relative closeness to the ideal solution

	Material specification	r_j (mean value)	S_j^+	S_j^-	C_j^+
Forgings (Matrix A)	ASME SA 533 Gr. B Cl.1	0.47	0.47	0.36	0.43
	JIS G-3120 SQV2A	0.36	0.58	0.25	0.30
	JPB	0.50	0.44	0.39	0.47
	JPC	0.57	0.37	0.46	0.55
Plates (Matrix B)	ASME SA-508 Cl.3	0.36	0.58	0.25	0.30
	KTA-DIN 20MnMoNi55	0.69	0.25	0.58	0.70
	RCC 16MND5	0.46	0.48	0.35	0.42
	JIS G-3204 SFVQ1A	0.36	0.58	0.25	0.30
	Material specification	r_j (mean value)	S_j^+	S_j^-	C_j^+
Inner cladding (Matrix C)	AISI 304L	0.35	0.59	0.24	0.29
	DIN X5 Cr Ni 18-10	0.35	0.59	0.24	0.29
	AISI 347	0.35	0.59	0.24	0.29
	DIN X6 Cr Ni Nb 18-10	0.72	0.22	0.61	0.73

According to the stringency level methodology, the best option for reactor pressure vessel manufacturing is the use of the forged material DIN 20MnMoNi55 along with the cladding DIN X6CrNiNb 18-10. This result enhances the modern practice of reactor pressure vessel manufacturing that consists of welding forged rings.
Fig. 13 provides the relative closeness to the ideal solution by manufacturing code or standard.

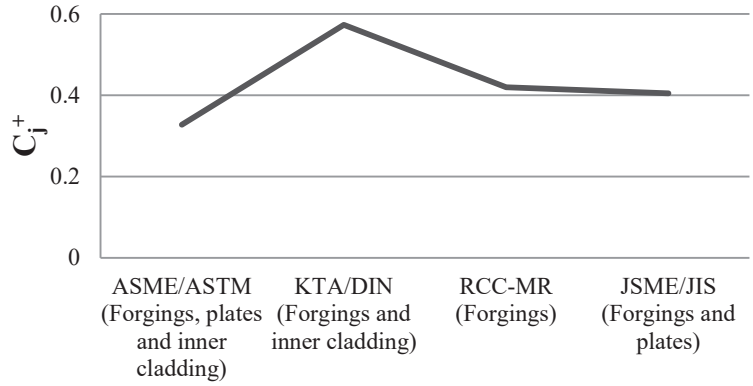

Fig. 13 Relative closeness to the ideal solution by the manufacturing code or standard

As the obtained value of C_j^+ (Table 8) and the Fig. 13 provide, the best option is the selection of German manufacturing standards to manufacture the reactor pressure vessel. Once obtained the final results through the multicriteria assessment using the threshold obtained by the multiobjective analysis of embrittlement and fracture prediction models for the base material and the inner cladding, a sensitivity analysis (Stage D) is performed to validate and analyze the integration of multicriteria decision making aspects into the stringency level methodology.

Stage D.- Sensitivity analysis and validation of the integrated multicriteria assessment

Performance of the proposed model is evaluated comparing the normalized outputs from the stringency level methodology versus the outputs obtained using the multicriteria (MCDM) approach. The sensitivity index (SI) of the output is determined using the Eqs. (38) and (39) based on the model proposed by Vijayaraghavan (2015).

$$L_i = | f_{SLM}(r_j) - f_{MCDM}(r_j) | \tag{38}$$

$$SI_j = \frac{L_j}{\sum_{j=1}^{n} L_j} \tag{39}$$

where $f_{SLM}(xi)$ and $f_{MCDM}(xi)$ are, respectively, the normalized values obtain using the stringency level methodology and the multicriteria decision making methodology.

Table 9 provides the sensitivity calculation using the concepts of $f_{SLM}(x_i)$ and $f_{MCDM}(x_i)$.

Table 9 Sensitivity calculation

	Material specification	$f_{MCDM}(x_i)$. $r_{j,\,MCDM}$ (mean value)	$f_{SLM}(x_i)$. $r_{j,\,SLM}$ (mean value)	L_i	SI_j	SI_i (mean)
ASME/ASTM	ASME SA 533 Gr. B Cl.1	0.47	0.30	0.17	0.11	0.06
	ASME SA-508 Cl.3	0.36	0.25	0.11	0.07	
	AISI 304L	0.35	0.32	0.03	0.02	
	AISI 347	0.35	0.32	0.03	0.02	
KTA/DIN	KTA-DIN 20MnMoNi55	0.69	0.45	0.24	0.16	0.09
	DIN X5 Cr Ni 18-10	0.35	0.32	0.03	0.02	
	DIN X6 Cr Ni Nb 18-10	0.72	0.57	0.15	0.10	
RCC-MR	RCC 16MND5	0.46	0.31	0.15	0.10	0.10
JSME/JIS	JIS G-3120	0.36	0.25	0.11	0.07	0.10
	JPB	0.50	0.34	0.16	0.11	
	JPC	0.57	0.34	0.23	0.15	
	JIS G-3204 SFVQ1A	0.36	0.25	0.11	0.07	
Mean (Total)						0.09

The results obtained (Table 9) exhibit that the sensitivity index varies between 0.06 (6%) for the ASME code/ASTM standards up to 0.10 (10%) for the JSME code/JIS standards and the RCC-MR code. The mean is approximately 0.09 (9%) and it could be considered as a reference measurement of the sensitivity of the proposed process (multicriteria stringency level methodology) with respect to the simple stringency level methodology, which does not consider dispersion among results.

4 Conclusions

A methodology for selecting a combination of materials specifications to manufacture reactor pressure vessels has been presented. This new approach considers the evaluation of materials requirements using a multicriteria stringency level methodology that defines several thresholds obtained analyzing different prediction models of embrittlement and fracture on low alloy steels and austenitic stainless steels operating in the reactor environment.

We have defined a multiobjective approach to solve the conflicts among thresholds as provided by different prediction models and certain constraints as described by different regulations for the base material and the inner cladding.

Applying the improved SL methodology using MCDM concepts, the best option is the selection of German manufacturing standards to manufacture the reactor pressure vessel and the material specification DIN 20MnMoNi55 for forged parts along with the DIN X6CrNiNb 18-10 for claddings. The sensitivity of the proposed process (multicriteria stringency level methodology) with respect to the customary stringency level methodology has been equal to 0.09, demonstrating that there is convergence between methodologies and a reduced variability.

The new methodology exhibits several improvements with respect to the customary stringency level methodology; since this novel approach considers multiple prediction models of irradiation embrittlement and hot cracking and it uses normalization vectors to allow us make a decision about the best option of material specification.

In the future, this methodology can be used in the analysis of different manufacturing codes or standards for other demanding applications.

References

Amayev, A.D., Kryukov, A.M., Sokov, M.A.: Recovery of the Transition Temperature of Irradiated WWER-440 Vessel Metal by Annealing, Steele, L.E. (ed.) Radiation Embrittlement of Nuclear Pressure Vessel Steels: An International Review (Fourth Volume), ASTM STP 1170, 369-379 (1993).

American Society for Metals – ASM: Source book on stainless steels. Engineering Bockshelfs, Russell Township,USA (2012).

Arantes F.M.L., Trevisan R.E.: Experimental and theoretical evaluation of solidification cracking in weld metal. Journal of achievements in Materials and Manufacturing engineering. 20(1-2), 407-410 (2007).

Asadi, M., Goldak, J.A., Nielsen J., Zhou, J., Tchernov, S., Downey, D.: Analysis of predicted residual stress in a weld and comparison with experimental data using regression model. Int. J. Mech. Mater. Des. 5, 353–364 (2009).

ASME B&PV II D App. 1 mandatory, 2015, Basis for establishing stress values. American Society of Mechanical Engineers, New York (2015).
ASME B&PV: Boiler and pressure vessels code. American Society of Mechanical Engineers, New York (2015).
ASTM E900: Standard Guide for Predicting Radiation-Induced Transition Temperature Shift in Reactor Vessel Materials. American Society for Testing and Materials, Philadephia (2002).
Ballesteros A., Acosta B.: Embrittlement trend curve for vessel steels with low copper content. International Atomic Energy Agency, Vienna (1997).
Blagoeva D.T., Debarberis L., Jong M., ten Pierick P.: Stability of ferritic steel to higher doses: Survey of reactor pressure vessel steel data and comparison with candidate materials for future nuclear systems. Int. J. Pres. Ves Pip. 122, 1-5 (2014).
Bringas J.E. (Ed.): Handbook of comparative world steel standards. American Society for Testing and Materials, Philadelphia (2000).
Brooks, A., Thompson, W.: Microstructural development and solidification cracking susceptibility of austenitic stainless steel welds. Int. Mater. Rev. 36, 16–44 (1991).
Chauhan, A., Vaish, R., Bowen, C.: Piezoelectric material selection for ultrasonic transducer and actuator applications. Proc IMechE Part L: J Materials: Design and Applications. 229 (1), 3–12 (2015).
Chung, H.M., Perry, D.L., Shack W.J.: Sulphur in austenitic stainless steel and irradiation assisted stress corrosion cracking. NACE International, Houston (2003).
Eason, E.D., Wright, J.E., Odette, G.R.: Improved embrittlement correlations for reactor pressure vessel steels, NUREG/CR-6551. U.S. Nuclear Regulatory Commission, Washington D.C (1998).
Fujii, K., Fukuya, K., Kasada, R., Kimura, A., Ohkubo, T.: Effects of stress on radiation hardening and microstructural evolution in A533B steel. J. Nucl. Mater. 407(3), 151–156(2010)
Gillemot, F.: Overview of reactor pressure vessel cladding. International Journal of Nuclear Knowledge Management. 4(4), 265–278 (2010).
Hyde, T., Sun, W.: Some issues on creep damage modelling of welds with heterogeneous structures. Int. J. Mech. Mater. Des. 5, 327–335 (2009).
IAEA: Earthquake preparedness and response for Nuclear Power Plants. International Atomic Energy Agency Publications, Vienna (2011).
Jenkins, M.L. Kirk, M.A., Pythian, W.J.: Experimental studies of cascade phenomena in metals. J. Nucl. Mater. 205, 16-30 (1993).
Jiang, C., Huang, X.P., Wei, X.P., Liu, N.Y.: A time-variant reliability analysis method for structural systems based on stochastic process discretization. Int. J. Mech. Mater. Des. 13, 173–193 (2017).
Kim M.C., Park S.G., Lee K.H., Lee, B.S.: Comparison of fracture properties in SA508 Gr.3 and Gr.4N high strength low alloy steels for advanced pressure vessel materials. Int. J. Pres. Ves Pip. 131, 60-66 (2015).
Kirk M.: Development of the alternate pressurized thermal shock rule (10 CFR 50.61a) in the United States. *Nucl. Eng. Technol.* 45(3), 277-294 (2013).
Kobayashi, S., Sato, H., Iwawaki, T., Yamamoto, T., Klingensmith, D., Odette, G.R., Kikuchi, H., Kamada, Y.: Effect of long-term thermal aging on magnetic property in reactor pressure vessel steels. J. Nucl. Mater. 439(1–3), 131-136 (2013).
Kobayashi, S., Yamamoto, T., Klingensmith, D., Odette, G.R., Kikuchi, H., Kamada Y.: Magnetic evaluation of irradiation hardening in A533B reactor pressure vessel steels: Magnetic hysteresis measurements and the model analysis. J. Nucl. Mater. 422(1–3), 158-162 (2012).
Kotecki, D., Sievert, T.A.: WRC-1992 Constitution diagram for stainless steel weld metal: a modification of the WRC –1988 diagram. Weld. J. 71, 171-178 (1992).
KTA Safety Standard 3201.1: Components of the Reactor Coolant Pressure Boundary of Light Water Reactors. Part 1: Materials and Product Forms. Nuclear Safety Standards Commission (KTA), Salzgitter (1998).
KTA Safety Standard 3201.3: Components of the reactor coolant pressure boundary of light water reactors - Part 3: manufacture". Nuclear Safety Standards Commission (KTA), Salzgitter (2007).
KTA Safety Standard 3203: Surveillance of the irradiation behaviour of reactor pressure vessel materials of LWR facilities". Nuclear Safety Standards Commission (KTA), Salzgitter (2001).
Kwon, J., Kwon, S.C., Hong J-H.: Prediction of radiation hardening in reactor pressure vessel steel based on a theoretical model. Ann. Nucl. Energy. 30(15), 1549-1559 (2003).
Leite, M., Silva, A., Henriques, E., Madeira, J.F.A.: Materials selection for a set of multiple parts considering manufacturing costs and weight reduction with structural isoperformance using direct multisearch optimization. Struct. Multidiscip. Optim. 52, 635-644 (2015).
Milani, A.S., Shanian, A.: Gear material selection with uncertain and incomplete data. Material performance indices and decision aid model. Int. J. Mech. Mater. Des. 3, 209–222 (2006).
Moorhead, A.J., Sikka, V.K., Reed, R.W.: Effect of small additions of niobium on the welding behaviour of an austenitic stainless steel, properties of austenitic stainless steels and their weld metals (influence of slaight chemistry variations*). ASTM Special Technical Publication.* 679, 103–111 (1979).
R. Kemp, G.A. Cottrell, H.K.D.H. Bhadeshia, G.R. Odette, T. Yamamoto, H. Kishimoto. Neural-network analysis of irradiation hardening in low-activation steels. J. Nucl. Mater. 348(3), 311-328 (2006).
RCC – MR.: Design and construction rules for mechanical components of nuclear installations applicable for high temperature structures and ITER vacuum vessel. AFCEN publications, Paris (2007).
Regulatory Guide R.G 1.99 Rev.1.: Effects of residual elements on predicted radiation damage to reactor vessels materials. Nuclear Regulatory Commission (NRC), Washington D.C (1977).
Regulatory Guide R.G 1.99 Rev.2.: Radiation Embrittlement of Reactor Vessel Materials. Nuclear Regulatory Commission, Washington D.C. (1988).
Riou, B., Escaravage, C., Hittner, D., Pierron, D.: Issues in reactor pressure vessel materials. In: Proceedings of the 2nd International Topical Meeting on High Temperature Reactor Technology, 22 – 24 September, Beijing (China), 10–22 (2004).
Rodríguez, A., Camacho, A.M., Sebastián, M.A.: Prediction of the Mechanical Behaviour of Cladding Materials for Nuclear Reactor Pressure–Vessels Based on the Analysis of Technological Requirements. Procedia Eng. 100, 1301–1308 (2015).
Rodríguez-Prieto, A., Camacho, A.M., Sebastián, M.A.: Materials selection criteria for nuclear power applications: a decision algorithm. JOM. 68(2), 496 – 506 (2016).

Rodríguez-Prieto, A., Camacho, A.M., Sebastián, M.A.: Selection of candidate materials for reactor pressure vessels: Application of irradiation embrittlement prediction models and a stringency level methodology. Proc IMechE Part L: J Materials: Design and Applications. DOI: 10.1177/1464420717727769 (2017a).

Rodríguez-Prieto, A., Camacho, A.M., Sebastián, M.A.: "Evaluation method for pressure vessel manufacturing codes: the influence of ASME unit conversion". Int. J. Mater. Prod. Technol. 54, (4), 259-274 (2017b).

Rodríguez-Prieto, A., Camacho, A.M., Sebastián, M.A.: "Quantitative analysis of prediction models of hot cracking in stainless steels using standardized requirements". Sadh. Acad. Proc. Eng. Sci. DOI: 10.1007/s12046-017-0745-2 (2017c).

Sharifian, M.: Nonlinear elastoplastic analysis of pressure sensitive materials. Int. J. Mech. Mater. Des. DOI 10.1007/s10999-017-9377-2 (2017).

Soneda, N., Dohi, K., Nishida, K., Nomoto, A., Iwasaki, M., Tsuno, S., Akiyama, T., Watanabe, S., Ohta, T.: Flux effect on neutron irradiation embrittlement of Reactor Pressure Vessel steels irradiated to high fluences. Proceedings of the International Symposium on Contribution of Materials Investigations to Improve the Safety and Performance of LWRs, 26 – 30 September, Avignon (France), 1 – 9 (2011).

Timofeev, B.: Assessment of the first generation RPV state after designed lifetime. Int. J. Pres. Ves Pip. 81(8), 703-712 (2004).

Valiente, M.A. Predictive and Measurement Methods for Delta Ferrite Determination in Stainless Steels. *Weld. J*. 91(4), 113-121 (2012).

Vijayaraghavan, V., Garg, A., Wong, C.H., Tai, K., Singru, P.M.: An integrated computational approach for determining the elastic properties of boron nitride nanotubes. Int. J. Mech. Mater. Des. 11, 1–14 (2015).

Welding Handbook: Materials and Applications Part 2. Nine Edition, Volume 4. American welding society (AWS) publications, Miami (2014).

Wu, S.J., Cao, L.W.: Effect of intergranular failure on the critical fracture stress and the fracture toughness of degraded reactor pressure vessel steel. Int. J. Pres. Ves Pip. 101, 23-29 (2013).